arXiv:1401.7357v3 [hep-ph] 6 Aug 2014

On Neutrino Masses in the MSSM with BRpV

Marco A. Díaz[a], Maximiliano A. Rivera[b] and Nicolás Rojas[a]

[a]*Departamento de Física, Universidad Católica de Chile,*
Avenida Vicuña Mackenna 4860, Santiago, Chile
[b]*Departamento de Física, Universidad Técnica Federico Santa María*
Casilla 110-V, Valparaiso, Chile

mad@susy.fis.puc.cl, maximiliano.rivera@usm.cl, nrojas1@uc.cl

Abstract

One loop corrections to the neutrino mass matrix within the MSSM with Bilinear R Parity Violation are calculated, paying attention to the approach in which an effective 3×3 neutrino mass matrix is used. The full mass matrix is block diagonalized, it is found that second and third order terms can be numerically important, and this is analytically understood. Top-stop loops do not contribute to the effective 3×3 at first order, nevertheless they contribute at third. An improved 3×3 approach that include these effects is proposed. A scan over parameter space is made supporting the conclusions.

1 Introduction

The evidence for neutrino oscillation comes from many experiments around the world [1–9]. The activity around neutrino physics has grown due to a more precise determination of neutrino oscillation parameters, specially coming from experiments connected with the reactor angle θ_{13} [10–14]. Global fits [15] using data from the mentioned experiments, allow to extract three mixing angles: two large θ_{21} and θ_{23}, one small θ_{13}, and two mass scales Δm^2_{21} and Δm^2_{32}. This information, constitutes an experimental evidence that the Standard Model (SM) must be extended.

If neutrinos are massive Majorana particles, lepton number violating terms must be present. In the Minimal Supersymmetric Standard Model (MSSM) [16] with Bilinear R-Parity Violation (BRpV) [17], R-parity is broken via lepton number violation, introducing a bilinear term at the superpotential level [18–21]. Therefore, neutrino masses and mixing angles are generated via a low-energy see-saw mechanism, mixing neutrino flavor-eigenstates

and neutralinos. Although this solution is appealing to explain neutrino masses and mixing angles, signals for supersymmetry at the LHC have not been seen [22]. Since the majority of the searches are based on supersymmetry with bilinear R-parity conserved, there is an open window for it.

In the MSSM with R-Parity violation, one neutrino mass is generated at tree-level, while the other two neutrinos remain massless. To reconcile theoretical predictions with the experimental data requires going beyond the tree-level approximation [23]. Several authors have shown the dependence of the neutrino masses in terms of the parameter which bilinearly violate R-parity, and also how to determine these from collider physics [24]. Improvements in the precision measurement of the neutrino parameters [25], as it will be discussed, suggest to go beyond one loop order in the calculation of the neutrino masses.

The most convenient way to numerically introduce one loop corrections to neutrino masses in this model is through the 7×7 mass matrix, which includes 4 neutralinos and 3 neutrinos. If this mass matrix is block diagonalized, an effective 3×3 neutrino mass matrix is generated, and it is very convenient when an algebraical understanding is sought. Nevertheless, the 3×3 approach can miss important numerical effects. This motivates a more careful treatment of the block diagonalization, leading to an improved 3×3 approach.

The paper is organized as follow: In section 2, introductory remarks about neutrino mass generation in BRpV are provided. Section 3 shows how loop corrections are treated in this article. Section 4 develops algebraic approximations that explain the numerical effects. Finally, conclusions about the findings are provided.

2 Neutrino Masses in Bilinear R-Parity Violation

Models with BRpV include a bilinear term in the superpotential that violates simultaneously R-Parity and lepton number. The superpotential has the following form,

$$W = W_{Yuk} + \varepsilon_{ab}\left(-\mu \widehat{H}_d^a \widehat{H}_u^b + \epsilon_i \widehat{L}_i^a \widehat{H}_u^b\right), \tag{2.1}$$

where in W_{Yuk} one has the usual R-Parity conserving (hereafter, RpC) Yukawa terms. Here the explicit bilinear terms are shown, with μ the higgsino mass and ϵ_i the BRpV mass parameters. In this work trilinear R-Parity violating terms are not considered, motivated by models that generate BRpV and not TRpV [26]. The terms shown in eq. (2.1) induce a mixing between neutralinos and neutrinos, forming a set of seven neutral fermions F_i^0. The corresponding tree level mass terms can be written by a 7×7 mass matrix as follows,

$$\mathcal{M}_N^0 = \begin{bmatrix} \mathrm{M}_\chi^0 & m^T \\ m & 0 \end{bmatrix}. \tag{2.2}$$

The sub-matrix M_χ^0 is the usual tree-level neutralino mass matrix of the MSSM, and m is the BRpV mixing matrix which mix neutralinos and neutrinos. Those are given by,

$$\mathrm{M}_\chi^0 = \begin{bmatrix} M_1 & 0 & -\frac{1}{2}g'v_d & \frac{1}{2}g'v_u \\ 0 & M_2 & \frac{1}{2}gv_d & -\frac{1}{2}gv_u \\ -\frac{1}{2}g'v_d & \frac{1}{2}gv_d & 0 & -\mu \\ \frac{1}{2}g'v_u & -\frac{1}{2}gv_u & -\mu & 0 \end{bmatrix} \quad ; \quad m = \begin{bmatrix} -\frac{1}{2}g'v_1 & \frac{1}{2}gv_1 & 0 & \epsilon_1 \\ -\frac{1}{2}g'v_2 & \frac{1}{2}gv_2 & 0 & \epsilon_2 \\ -\frac{1}{2}g'v_3 & \frac{1}{2}gv_3 & 0 & \epsilon_3 \end{bmatrix}. \tag{2.3}$$

The matrix m includes the sneutrino vacuum expectation values v_i. These vev's appear induced by the ϵ_i in the superpotential as well as by the corresponding soft bilinear terms, not shown in this article (for more details, see [20, 27]). Eq. (2.2) can be block-diagonalized using the rotation matrix,

$$\mathbf{R}_{bd}^0 = \begin{bmatrix} 1 - \frac{1}{2}\xi^T\xi & \xi^T \\ -\xi & 1 - \frac{1}{2}\xi\xi^T \end{bmatrix}, \tag{2.4}$$

with $\xi = m\,\mathrm{M}_\chi^{0\,-1}$. In this way, the block-diagonal mass matrix is,

$$\begin{aligned} \mathcal{M}_N^{bd,0} &= \begin{bmatrix} \mathrm{M}_\chi^0 + \frac{1}{2}(m^T m\,\mathrm{M}_\chi^{0\,-1} + \mathrm{M}_\chi^{0\,-1} m^T m) & 0 \\ 0 & -m\,\mathrm{M}_\chi^{0\,-1}\,m^T \end{bmatrix} \\ &\equiv \begin{bmatrix} \mathrm{M}_\chi^{bd,0} & 0 \\ 0 & \mathrm{M}_\nu^{bd,0} \end{bmatrix}. \end{aligned} \tag{2.5}$$

The correction in the neutralino sector is usually ignored, while the correction in the neutrino sector is the well known tree-level neutrino effective mass matrix,

$$\mathbf{M}_\nu^{bd,0} = -m\,\mathrm{M}_\chi^{0\,-1}\,m^T = \frac{M_1 g^2 + M_2 g'^2}{4\det \mathrm{M}_\chi^0} \begin{bmatrix} \Lambda_1^2 & \Lambda_1\Lambda_2 & \Lambda_1\Lambda_3 \\ \Lambda_2\Lambda_1 & \Lambda_2^2 & \Lambda_2\Lambda_3 \\ \Lambda_3\Lambda_1 & \Lambda_3\Lambda_2 & \Lambda_3^2 \end{bmatrix}, \tag{2.6}$$

with $\Lambda_i = \mu v_i + \epsilon_i v_d$. The matrix clearly has only one eigenvalue different from zero, which is experimentally unacceptable.

It is known that this problem is solved by radiative corrections. Concentrating only on loops with neutrinos in the external legs, one has for example,

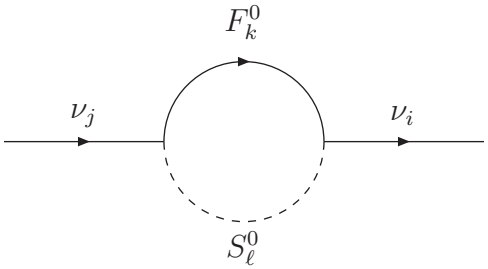

where F_k^0 are the mentioned neutral fermions and S_ℓ^0 are scalars formed by the mixing between Higgs bosons and sneutrinos [20]. These contributions can be calculated approximately in the block-diagonalized basis, obtaining a generalization to the neutrino mass matrix in eq. (2.6), which is customary to write as,

$$\left[\mathbf{M}_\nu^{bd(1)}\right]_{ij} = A\,\Lambda_i\Lambda_j + B\big(\Lambda_i\epsilon_j + \Lambda_j\epsilon_i\big) + C\,\epsilon_i\epsilon_j\,, \tag{2.7}$$

where the parameter A receives tree-level contributions given in eq. (2.6), while the parameters B and C are loop generated. It is also worth mentioning that the parameter C is scale invariant, while B is not.

As mentioned, the neutrino/neutralino tree-level mass matrix is completely diagonalized. This is done by applying an extra rotation to the one shown in eq. (2.4). This is,

$$\mathbf{R}_{xd}^0 = \left[\begin{array}{cc} N & 0 \\ 0 & N_\nu \end{array}\right]. \tag{2.8}$$

The matrix N_ν diagonalizes the effective tree-level neutrino mass matrix given in eq. (2.6) [21], and the N matrix diagonalizes the 4×4 neutralino mass matrix. The net effect is to have,

$$\mathcal{M}_N^{d,0} = \mathbf{R}_{xd}^0\,\mathbf{R}_{bd}^0\,\mathcal{M}_N^0\,\mathbf{R}_{bd}^{0T}\,\mathbf{R}_{xd}^{0T} = \left(\begin{array}{cc} \mathrm{M}_\chi^{d,0} & 0 \\ 0 & \mathrm{M}_\nu^{d,0} \end{array}\right). \tag{2.9}$$

It is at this point that quantum corrections are included,

$$\mathcal{M}_N^1 = \mathcal{M}_N^{d,0} + \Delta\mathcal{M}_N^1 \;\; = \;\; \left(\begin{array}{cc} \mathrm{M}_\chi^{d,0} + \delta M_\chi & \delta m^T \\ \delta m & \mathrm{M}_\nu^{d,0} + \delta M_\nu \end{array}\right), \tag{2.10}$$

where δM_χ are one-loop corrections within the neutralino 4×4 sub-matrix, δM_ν the one-loop corrections to the 3×3 neutrino sub-matrix, and δm refers to the one-loop corrections to the neutralino/neutrino mixing sector. The above matrix can be block-diagonalized again, obtaining the following result,

$$\mathcal{M}_N^{bd,1} = \left[\begin{array}{cc} \mathrm{M}_\chi^{bd,1} & 0 \\ 0 & \mathrm{M}_\nu^{bd,1} \end{array}\right], \tag{2.11}$$

where there have been defined,

$$\mathrm{M}_\nu^{bd,1} = \mathrm{M}_\nu^{d,0} + \delta M_\nu - \delta m\,(\mathrm{M}_\chi^{d,0})^{-1}\,\delta m^T + \delta m\,(\mathrm{M}_\chi^{d,0})^{-1}\,\delta M_{\tilde{\chi}}\,(\mathrm{M}_\chi^{d,0})^{-1}\delta m^T \tag{2.12}$$

and

$$\mathrm{M}_\chi^{bd,1} = \mathrm{M}_\chi^{d,0} + \delta M_\chi \tag{2.13}$$

Notice that the last two terms in equation (2.12) are of second and third order in our block-diagonalization expansion, and thus they are susceptible to be neglected. Nevertheless, since the neutrino masses are several orders of magnitude smaller than the neutralino masses, the two terms are numerically important.

Parameter	Value	Units
$\tan\beta$	16.7	-
μ	3171	GeV
M_1	409	GeV
M_2	587	GeV
M_3	5240	GeV
M_Q	4436	GeV
M_U	4037	GeV
M_D	4668	GeV
M_L	1668	GeV
M_R	1964	GeV

Table 1: Supersymmetric parameters at the renormalization scale $Q = 4233$ GeV. Sfermion mass parameters are given for the third generation.

Particle	Mass
h	126
A	3168
χ_1^0	405
χ_1^+	626
$\tilde{\nu}_\tau$	1667
$\tilde{\tau}_1$	1666
$\tilde{t}_1$	4142
$\tilde{b}_1$	4583

Table 2: Part of the supersymmetric spectrum (in GeV).

3 High Order Effects on Neutrino Masses

In order to show these effects, one-loop corrected neutrino masses in a specific supersymmetric scenario are calculated. A few of the parameters that define this benchmark are shown in Table 1, where the given scalar masses correspond to the third generation. In addition, in Table 2 are shown the masses of a few relevant particles. This scenario was generated using the code SUSPECT [28] for the RpC part. In particular, the Higgs boson mass is 126 GeV, as measured by experiments [29]. In addition, SUSPECT allows the calculation for: (i) the deviation from unity of the ρ parameter $\Delta\rho = 7.7 \times 10^{-6}$ [30,31], (ii) the anomalous magnetic moment of the muon $\Delta a_\mu = 5.7 \times 10^{-11}$ [30,32], and (iii) the branching ratio for the radiative decay of a bottom quark $B(b \to s\gamma) = 3.3 \times 10^{-4}$ [33].

The BRpV part is handled by our own code. Since BRpV parameters are much smaller

Parameter	Value	Units
ϵ_1	0.162	GeV
ϵ_2	-0.043	GeV
ϵ_3	0.192	GeV
Λ_1	0.153	GeV^2
Λ_2	0.178	GeV^2
Λ_3	0.067	GeV^2

Table 3: BRpV parameters.

Observable	Central Value	3σ exp. value	Units
Δm^2_{atm}	2.56×10^{-3}	$2.31 - 2.74 \times 10^{-3}$	eV^2
Δm^2_{sol}	7.62×10^{-5}	$7.12 - 8.20 \times 10^{-5}$	eV^2
$\sin^2\theta_{atm}$	0.639	$0.36 - 0.68$	-
$\sin^2\theta_{sol}$	0.305	$0.27 - 0.37$	-
$\sin^2\theta_{rea}$	0.024	$0.017 - 0.033$	-

Table 4: Experimental neutrino observables.

than the supersymmetric scale represented by the Higgsino mass parameter μ, the extra contributions to the above loop quantities from BRpV are negligible. The selected BRpV parameters are given in Table 3. Note that the values for ϵ_i are large enough to make the radiative corrections to neutrino masses very important. The experimental values for the neutrino parameters are given in Table 4.

First of all, a study on how important are the different loops in the determination of the neutrino parameters has been performed. In Fig. 1 one works in the plane formed by the atmospheric Δm^2_{23} and the solar Δm^2_{12} neutrino mass parameters. In vertical and horizontal dashed lines the 3σ experimental limits for these parameters are shown. At approximately the center of this allowed region one has the predictions from our scenario using the full 7×7 mass matrix, represented by a dark (black) diamond. Flowing from this point one has several arrows ending in circles (red), one for each loop. What it is done here is to omit in every entry of the 7×7 mass matrix the contribution from the corresponding loop, and show the prediction for the mass differences in these conditions.

The contributions from the bottom-sbottom, neutralino-neutral scalar, and chargino-charged scalar loops are large as expected (Fig. 1-top). The not-so-known effect is the importance of the top-stop loops, which are large enough to move the prediction outside the 3-σ region when it is not included (Fig. 1-bottom). The reason for the unexpectedness of this result is that these loops do not contribute to the neutrino masses in the 3×3 approach, which is very popular. The contribution by these loops appears through the last term in eq. (2.12),

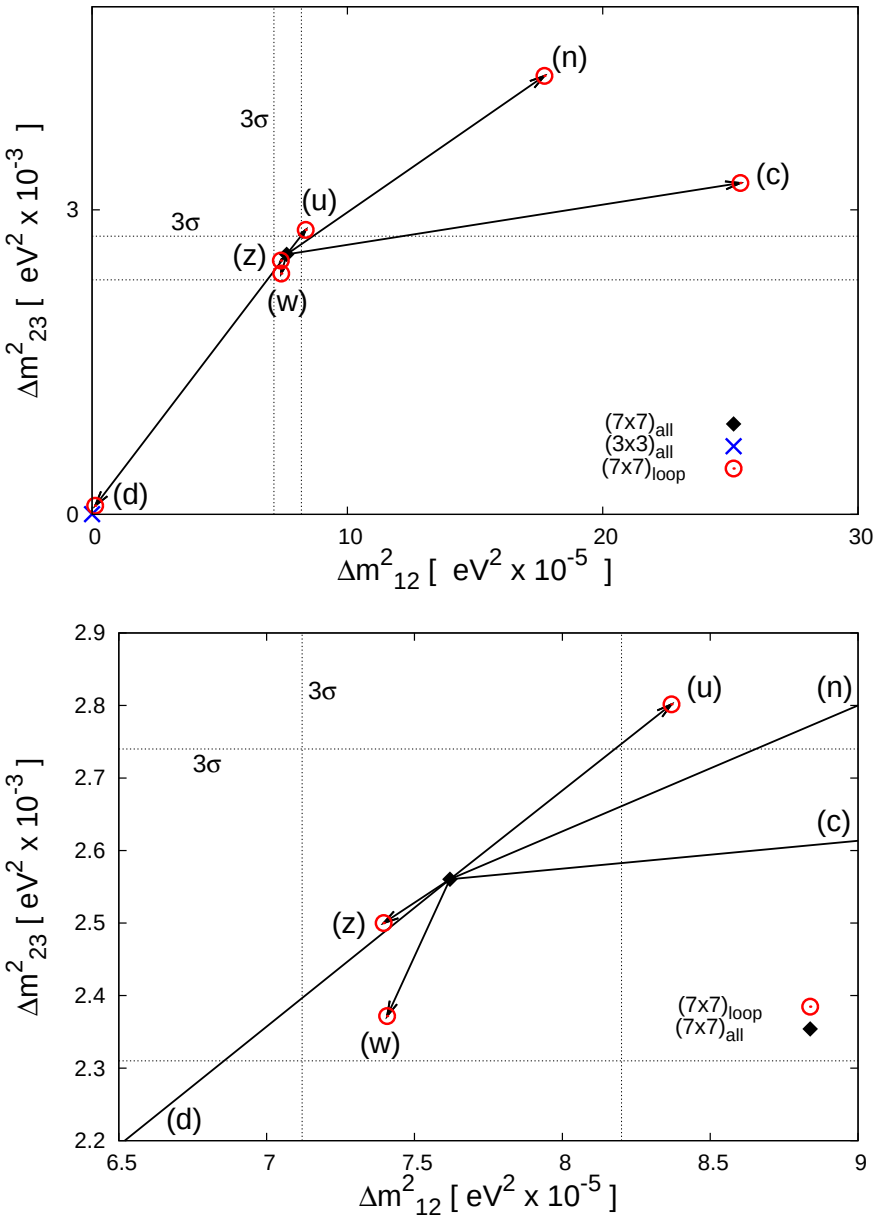

Figure 1: Influence of loop corrections on Δm^2_{atm} and Δm^2_{sol} in the whole 7×7 mass matrix. The lower figure is a zoom-in of the top one.

which is of third order. As explain in the next section, this contribution is proportional to the top quark Yukawa coupling and needs the presence of the bottom-sbottom loops as well. One may also see that in this particular scenario, the 3×3 approximation does not work since it gives a prediction for the solar and atmospheric mass squared parameters which are

off by several orders of magnitude, represented by a cross (blue).

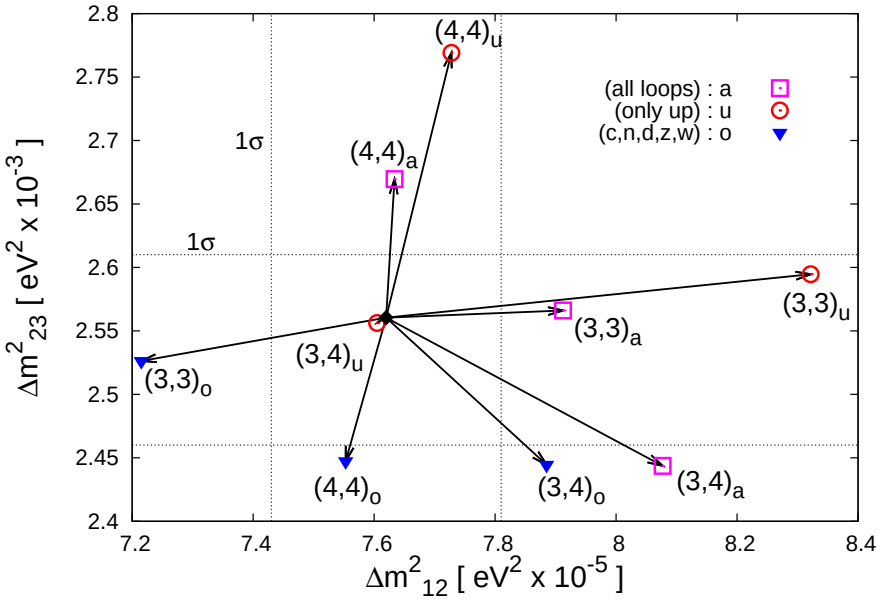

Figure 2: Influence of loop corrections on Δm^2_{atm} and Δm^2_{sol} in a given matrix element of the 7×7 mass matrix.

Second of all, in Fig. 2 a similar process is performed. This time a specific loop in a given entry in the 7×7 mass matrix is omitted. For the arrows ending in a square (magenta), one is omitting all the loops at each $(3,3)$, $(3,4)$ and $(4,4)$ matrix elements. For the arrows ending in a circle (red), one is omitting the up-sup loops for the same matrix elements. Finally, for the arrows ending in a triangle (blue), one is omitting all the loops except up-sup, also for the same matrix elements. The lesson draw from the figure is that the importance of the top-stop loops lies in the higgsino section of the mass matrix. This is clear since the corrections in that sector are proportional to the top quark Yukawa coupling.

When it is convenient to work with a 3×3 neutrino mass matrix, the second and third order terms in eq. (2.12) should be included, because they are numerically important. Once that is done, the precision obtained with the 7×7 approach is recovered. In Table 5 the prediction for the neutrino observables in the same scenario introduced before is shown. In the second and third column the usual 7×7 and 3×3 approaches are shown. In the last column the extra terms in eq. (2.12), calling the approach as $3 \times 3_{full}$, is included. It is clear the recovery in precision.

The second order is given by the third term in eq. (2.12). In the chosen scenario, this term is also very important. That can be understood from Fig. 1-top and Fig. 2. In Fig. 1-top the effect of the first order is seen by the cross (blue). The fact that this prediction is so small is an indication that this first order effect is also small. On the other hand, the effect

Observable	7×7	3×3	$3 \times 3_{full}$
Δm^2_{atm}	2.56×10^{-3}	2.02×10^{-6}	2.56×10^{-3}
Δm^2_{sol}	7.62×10^{-5}	1.53×10^{-8}	7.57×10^{-5}
$\sin^2\theta_{atm}$	0.639	0.839	0.640
$\sin^2\theta_{sol}$	0.305	0.442	0.303
$\sin^2\theta_{rea}$	0.024	0.407	0.024

Table 5: Neutrino observables calculated in the different approaches.

of the third order seen in Fig. 2, although large when compared to experimental errors, is small compared to full expansion (first plus second plus third order), therefore, the second order is very important.

4 Algebraic Approximations

Here, approximated algebraic expressions for second and third order terms from the top-stop contribution to the solar mass are found, in order to better understand the numeric results shown in the previous section. These numerical calculations show that top-stop loops contribute importantly.

The contribution from top-stop loops to the second order term in eq. (2.12) is studied. In the higgsino sector the relevant matrix elements of the inverse neutralino mass matrix, following the Appendix B is,

$$(\mathrm{M}^0_\chi)^{-1}_{34} = (\mathrm{M}^0_\chi)^{-1}_{43} \approx -\frac{1}{\mu}. \tag{4.14}$$

Therefore,

$$-\left[\delta m\, \mathrm{M}^{-1}_{\chi^0}\, \delta m^T\right]_{ij} \;=\; \frac{1}{\mu}\left[\delta m_{i3}\delta m_{j4} + \delta m_{i4}\delta m_{j3}\right]_{ij} = \frac{1}{\mu}(\delta m^{t\tilde{t}}_{3,\Lambda})(\delta m^{t\tilde{t}}_{4,\Lambda})\,\Lambda_i\Lambda_j\,, \tag{4.15}$$

and it does not contribute to the solar mass, since it is proportional to $\Lambda_i\Lambda_j$. In fact, since the top-stop coupling to neutrinos does not include ϵ terms, none of the quantities $\delta m^{t\tilde{t}}_{ij}$ will produce a contribution to the solar mass. Thus, third order term is studied next.

The third order term in eq. (2.12), given by

$$\delta m\,(\mathrm{M}^{d,0}_\chi)^{-1}\,\delta M_\chi\,(\mathrm{M}^{d,0}_\chi)^{-1}\delta m^T\,, \tag{4.16}$$

is written in the basis where the tree-level neutralino mass matrix has already been diagonalized. If work is to be done in the original basis instead, the term to analyze is,

$$\delta m\,(\mathrm{M}^0_\chi)^{-1}\,\delta M_\chi\,(\mathrm{M}^0_\chi)^{-1}\delta m^T\,, \tag{4.17}$$

where δm (and $\delta M_{\tilde{\chi}}$) in eq. (4.16) is written in the diagonal basis, while δm (and $\delta M_{\tilde{\chi}}$) in eq. (4.17) is written in the original basis. The same notation is used for both out of simplicity.

In order to algebraically understand the issues mentioned in the previous section a few approximations are performed. First, notice that down-type quarks contribute to δm with a term proportional to ϵ_i, while up-type quarks do not, as can be seen from the Appendix A. Thus, in this approximation,

$$(\delta m)_{ij} = \delta m_{i3}\, \delta_{j3}. \tag{4.18}$$

Second, notice that the $(4,4)$ matrix element in the neutralino sector makes a strong numerical effect on the neutrino parameters, and up-type quarks contribute to it. To isolate this effect it is assumed,

$$(\delta M_\chi)_{ij} = \delta M_{\chi,44}\, \delta_{i4}\, \delta_{j4}. \tag{4.19}$$

With this, the contribution from top-stop loops to the third order term in eq. (2.12) is,

$$\begin{aligned}
\left[\delta m\, (\mathrm{M}^0_\chi)^{-1}\, \delta M_\chi\, (\mathrm{M}^0_\chi)^{-1}\, \delta m^T\right]_{ij} &\approx \delta M^{t\tilde{t}}_{\chi,44}\, (\mathrm{M}^0_\chi)^{-2}_{34} (\delta m^{b\tilde{b}}_{i3})\, (\delta m^{b\tilde{b}}_{j3}) \qquad (4.20)\\
&\approx \delta M^{t\tilde{t}}_{\chi,44}\, (\mathrm{M}^0_\chi)^{-2}_{34} \Big[\delta m^{b\tilde{b}}_{3,\Lambda}\Lambda_i + \delta m^{b\tilde{b}}_{3,\epsilon}\epsilon_i\Big]\Big[\delta m^{b\tilde{b}}_{3,\Lambda}\Lambda_j + \delta m^{b\tilde{b}}_{3,\epsilon}\epsilon_j\Big].
\end{aligned}$$

Approximating further the $\epsilon\epsilon$ term is,

$$\begin{aligned}
\left[\delta m\, (\mathrm{M}^0_\chi)^{-1}\, \delta M_\chi\, (\mathrm{M}^0_\chi)^{-1}\, \delta m^T\right]^{\epsilon\epsilon}_{ij} &\approx \left[\frac{n_c h_t^2}{32\pi^2}\times 2\times 2\mu\right]\left[-\frac{1}{\mu}\right]^2\left[\frac{n_c h_b^2}{64\pi^2\mu}\times 2\times 2\mu\right]^2 \epsilon_i\epsilon_j\\
&= \frac{2 n_c^3 h_t^2 h_b^4}{(16\pi^2)^3\mu}\epsilon_i\epsilon_j \approx \frac{n_c^3 g^6 m_t^2 m_b^4}{4(16\pi^2)^3 s_\beta^2 c_\beta^4 m_W^6 \mu}\epsilon_i\epsilon_j\\
&\approx 10^{-2}\frac{t_\beta^4 \epsilon_i\epsilon_j}{\mu}\ \mathrm{eV}\,, \qquad (4.21)
\end{aligned}$$

which gives the same order of magnitude of the solar mass squared difference, thus it should not be neglected.

5 General Scan over Parameter Space

In order to see the 0 of the different approximations a general scan over the parameter space was made. As it was explained in section 3 the code SUSPECT [28] was used for the running of the RpC supersymmetric parameters, and our own code for the neutrino observables from the R-Parity violating parameters (since R-Parity violation is small, the use of MSSM RGEs for the RpC parameters is a good approximation). Randomly selected values for the RpC parameters at the GUT scale are generated and SUSPECT is used to find their counterpart at the weak scale, including a correct electroweak symmetry breaking. At this point the following cuts are added: the Higgs mass, $124 < m_h < 126$ GeV, $\Delta\rho$, Δa_μ, $B(b\to s\gamma)$ (see

Parameter	Minimum	Maximum	Units
$\tan\beta$	9.11	48.8	-
μ	655	4495	GeV
M_1	313	897	GeV
M_2	567	1597	GeV
M_3	3296	5952	GeV
M_Q	2862	6093	GeV
M_U	1616	5834	GeV
M_D	2427	6458	GeV
M_L	1007	5176	GeV
M_R	1024	4899	GeV
ϵ_1	-0.117	0.158	GeV
ϵ_2	-0.235	0.303	GeV
ϵ_3	-0.156	0.277	GeV
Λ_1	-0.102	0.112	GeV^2
Λ_2	-0.118	0.124	GeV^2
Λ_3	-0.130	0.116	GeV^2

Table 6: Intervals for each parameters at the low scale.

first paragraph in section 3). Then, randomly generated values for the RpV parameters are added to the 0 parameters, and with all of them a seed point in parameter space at the weak scale is defined. Using an implementation of the Markov chain [34] and starting from the seed point just described, a movement in steps is implemented, minimizing a χ^2 function that includes neutrino experimental parameters only (mass squared differences and mixing angles) towards a final point that satisfy neutrino physics. Finally, cuts on the masses of the following supersymmetric particles are implemented $m_{\chi_1^+} > 600$ GeV, $m_{\chi_1^0} > 300$ GeV, $m_{\tilde{\ell}} > 1$ TeV, $m_{\tilde{q}} > 2$ TeV, $m_{\tilde{g}} > 2$ TeV [35, 36]

Following section 3, some of the parameters at the weak scale that define the points that satisfy all cuts lie in intervals described in Table 6. Similarly, the interval for some of the physical masses are indicated in Table 7. The high value for the squark masses (and soft mass parameters as well) is due to the Higgs mass, which needs high squarks masses in order to reach the value $m_h \sim 125$ GeV. For the same reason (although contributing at two loops), the gluino mass is also high: $m_{\tilde{g}} > 3500$ GeV including radiative corrections.

In Fig. 3 the 0 of the 3×3 approximation in the μ-$\tan\beta$ plane is shown. Different colors according to the ratio $\Delta m^2_{sol(3\times3)}/\Delta m^2_{sol(7\times7)}$ are displayed (in principle), *i.e.*, the solar mass squared difference calculated with the 3×3 approximation in comparison with the same neutrino observable calculated with the full 7×7 matrix. It is seen that the solar mass calculated with the 3×3 approximation is always off by more than 50%. In fact, it is observed in the scan that it is always smaller, and very often the error is much larger than

Particle	Minimum	Maximum
h	124	126
A	1097	4128
χ_1^0	310	897
χ_1^+	601	1651
$\tilde{\nu}_\tau$	1005	5176
$\tilde{\tau}_1$	1001	4800
$\tilde{t}_1$	2973	6234
$\tilde{b}_1$	3216	6559

Table 7: Part of the supersymmetric spectrum (in GeV).

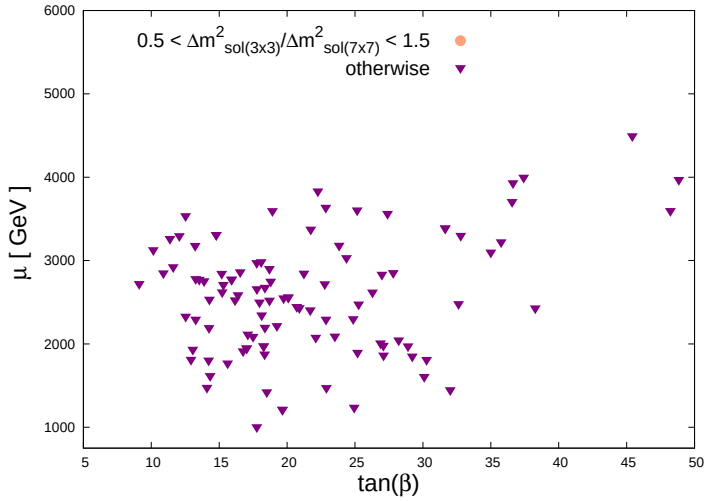

Figure 3: Solar mass squared difference calculated with the 3×3 approximation, in comparison with the one calculated with the 7×7 matrix.

50%. Considering the experimental errors in the measurement of the solar mass, the 3×3 approximation is not reliable anymore.

In Fig. 4 a similar comparison is made, but this time for the solar mass calculated with the $3 \times 3_{full}$ approximation. Furthermore, displayed are four quadrants that refer to four different values for the error: 0.1%, 1%, 2%, and 5%. In the lower-right frame (5%) it is seen that the $3 \times 3_{full}$ approximation is much better than the usual 3×3: almost all the time the solar mass lies within 5% with respect to the calculated with the 7×7 matrix. At the level of 0.1% (upper-left), even the $3 \times 3_{full}$ approximation fails in comparison with 7×7. In addition, from the sequence of frames in Fig. 4 it can be concluded that the $3 \times 3_{full}$ is more reliable at high values of $\tan\beta$. This can be understood from the fact that at high values of

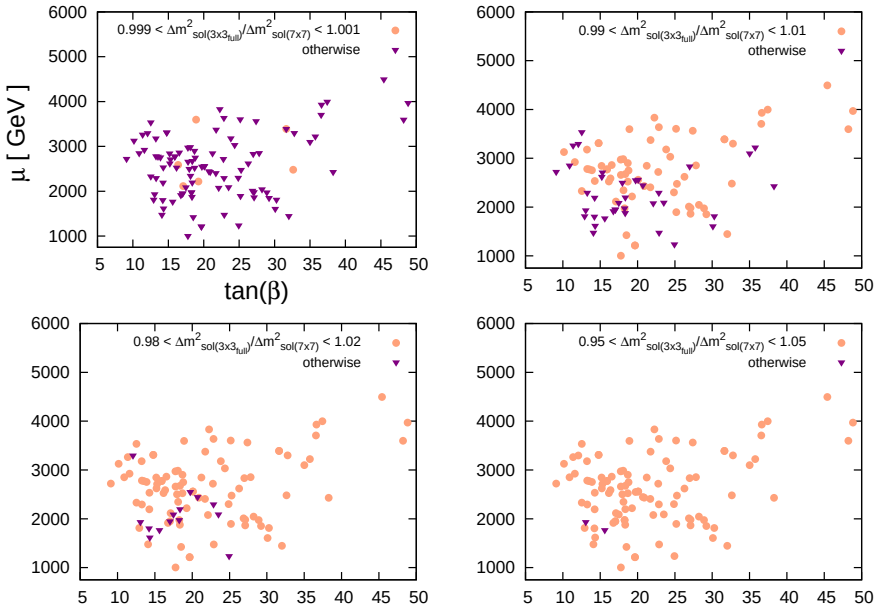

Figure 4: Solar mass squared difference calculated with the $3 \times 3_{full}$ approximation, in comparison with the one calculated with the 7×7 matrix.

$\tan\beta$ the bottom quark Yukawa coupling is larger and, therefore, bottom quark effects are more 0. This makes the $3 \times 3_{full}$ approximation more reliable, and simultaneously the 3×3 approximation less reliable, at high values of $\tan\beta$.

Finally in Fig. 5 it is seen the effect of the up type quarks and squarks on the solar mass, displayed in the same $\mu - \tan\beta$ plane. Notice that these loops contribute to the solar mass only via the third order term. In the scan the effect of removing all together the up-sup loops from the 7×7 matrix is shown, and a 0 with the solar mass calculated with the full 7×7 matrix is done. In most of the points the effect of the up-sup loops is large (larger than 5% in the figure).

6 Conclusions

It was shown that the 3×3 approach in the calculation of neutrino masses in the MSSM with BRpV, in the light of the present accuracy of the experimental results, sometimes does not give an acceptable answer. This was understood by studying the 3×3 second and third order terms in the block diagonalization of the 7×7 mass matrix. When it is convenient to work with 3×3 matrices, it was shown also that keeping these terms gives a very similar result compared to the ones extracted from the 7×7 neutrino mass matrix. In addition, in the 3×3 approach, the top-stop loops do not contribute, nevertheless, they can be numerically

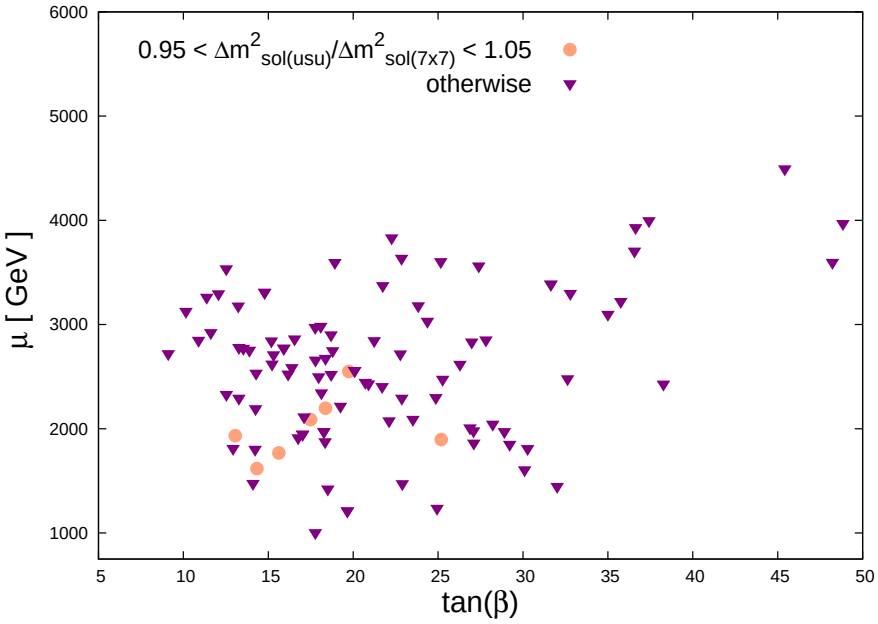

Figure 5: Effect of the removal of the up-type quark and squark loops.

important. These loops contribute through the already mentioned third order term, and it was shown that the contribution is dependent on the bottom as well as the top quark Yukawa couplings. The second order term in eq. (2.12) can also be very important. In fact, a scenario was chosen where it is crucial. All these issues motivate a two-loop calculation of neutrino masses in this model. A scan over parameter space is made to show that the conclusions are general, and not driven by the chosen point shown in section 3. Most of these numerical effect come from the high value of the Higgs boson mass.

Acknowledgments

This work was supported by Fondecyt grants No. 11110472, 1100837 and 1141190, Anillo "AtlasAndino" ACT1102, UTFSM-DGIP grant No. 11.12.39, and Conicyt Doctorate Grant.

A Squark Loop Contributions

A.1 Top-stop loops in δM_χ

It is numerically observed that among the 16 matrix elements of δM_χ, the $(4,4)$ is the one that gives the largest contribution. In addition, the top-stop loops have an important effect on this matrix element. In order to algebraically understand the phenomena, this contribution is calculated. The coupling between neutral fermions and top-stop quarks is,

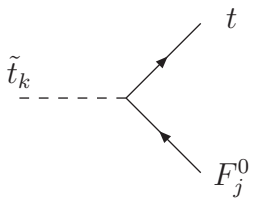

$$= i\left[O_{Ljk}^{tn\tilde{t}}\frac{(1-\gamma_5)}{2} + O_{Rjk}^{tn\tilde{t}}\frac{(1+\gamma_5)}{2}\right],$$

with

$$\begin{aligned} O_{Ljk}^{tn\tilde{t}} &= \eta_j \frac{4gt_W}{3\sqrt{2}}\mathcal{N}_{j1}^* R_{k2}^{\tilde{t}} - \eta_j h_t \mathcal{N}_{j4}^* R_{k1}^{\tilde{t}}\,, \\ O_{Rjk}^{tn\tilde{t}} &= -\frac{g}{\sqrt{2}}\left(\mathcal{N}_{j2} + \frac{1}{3}t_W\mathcal{N}_{j1}\right)R_{k1}^{\tilde{t}} - h_t\mathcal{N}_{j4}R_{k2}^{\tilde{t}}\,, \end{aligned} \tag{1.22}$$

and where h_t is the top quark Yukawa coupling, $R^{\tilde{t}}$ is the (assumed real) 2×2 rotation matrix that diagonalizes the stop quark mass matrix, $\mathcal{N}$ is the (assumed real) 7×7 rotation matrix that diagonalizes the neutralino sector, and η_j is the sign of the corresponding fermion j. Notice that the complex conjugated $\mathcal{N}^*$ is kept only for reference, since one assumes it is real. If this coupling is specialized to the case when the neutral fermion is a neutralino one finds,

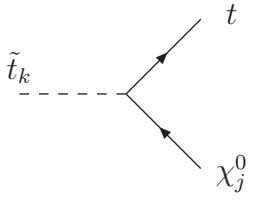

$$= i\left[O_{Ljk}^{t\chi\tilde{t}}\frac{(1-\gamma_5)}{2} + O_{Rjk}^{t\chi\tilde{t}}\frac{(1+\gamma_5)}{2}\right],$$

with

$$\begin{aligned} O_{Ljk}^{t\chi\tilde{t}} &= \eta_j \frac{4gt_W}{3\sqrt{2}}N_{j1}^* R_{k2}^{\tilde{t}} - \eta_j h_t N_{j4}^* R_{k1}^{\tilde{t}}\,, \\ O_{Rjk}^{t\chi\tilde{t}} &= -\frac{g}{\sqrt{2}}\left(N_{j2} + \frac{1}{3}t_W N_{j1}\right)R_{k1}^{\tilde{t}} - h_t N_{j4}R_{k2}^{\tilde{t}}\,. \end{aligned} \tag{1.23}$$

In this case, N is the (real) 4×4 rotation matrix that diagonalizes the neutralino mass sub-matrix, and η_j is the sign of the j-th neutralino mass. The relevant loop is formed with those couplings,

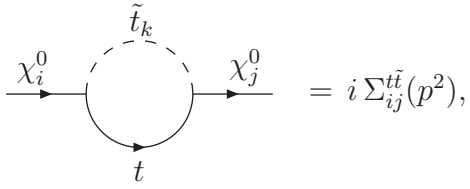

$$= i\,\Sigma_{ij}^{t\tilde{t}}(p^2),$$

with,

$$\Sigma_{ij}^{t\tilde{t}}(p^2) = \frac{n_c h_t^2 N_{i4} N_{j4}}{16\pi^2} \sum_{k=1}^{2} \left[m_t R_{k1}^{\tilde{t}} R_{k2}^{\tilde{t}} (\eta_i P_L + \eta_j P_R) B_0^{pt\tilde{t}} - \not{p} (R_{k1}^{\tilde{t}2} \eta_i \eta_j P_L + R_{k2}^{\tilde{t}2} P_R) B_1^{pt\tilde{t}} \right] + ... \tag{1.24}$$

Here the three dots mean that only the terms proportional to h_t^2 are shown. Also, the fact that the matrix N is real was already used.

When evaluating δM_χ^{ij} it should be understood that in the basis where the neutralinos are diagonal, one wants to evaluate the neutralino mass at p^2, and symmetrize over i and j. Thus,

$$\begin{aligned}
\delta M_\chi^{ij} &= \frac{n_c h_t^2 N_{i4} N_{j4}}{32\pi^2} \sum_{k=1}^{2} \Bigg\{ -\frac{1}{2} m_t R_{k1}^{\tilde{t}} R_{k2}^{\tilde{t}} (\eta_i + \eta_j) \left(B_0^{\chi_i t\tilde{t}} + B_0^{\chi_j t\tilde{t}} \right) \\
&\qquad + \frac{1}{2} (R_{k1}^{\tilde{t}2} \eta_i \eta_j + R_{k2}^{\tilde{t}2}) \left(m_{\chi_i^0} B_1^{\chi_i t\tilde{t}} + m_{\chi_j^0} B_1^{\chi_j t\tilde{t}} \right) \Bigg\}, \\
&= \frac{n_c h_t^2 N_{i4} N_{j4}}{32\pi^2} \sum_{k=1}^{2} \Bigg\{ \frac{1}{2} m_t s_{\tilde{t}} c_{\tilde{t}} (-1)^k (\eta_i + \eta_j) \left(B_0^{\chi_i t\tilde{t}} + B_0^{\chi_j t\tilde{t}} \right) \\
&\qquad + \frac{1}{2} (c_{\tilde{t}}^2 \eta_i \eta_j + s_{\tilde{t}}^2) \left(m_{\chi_i^0} B_1^{\chi_i t\tilde{t}} + m_{\chi_j^0} B_1^{\chi_j t\tilde{t}} \right) \Bigg\}.
\end{aligned} \tag{1.25}$$

The contribution to the $(4,4)$ neutrino/neutralino mass matrix element is therefore,

$$\delta M_\chi^{44} = \frac{n_c h_t^2 N_{44}^2}{32\pi^2} \sum_{k=1}^{2} \left\{ 2 m_t s_{\tilde{t}} c_{\tilde{t}} (-1)^k \eta_4 B_0(m_{\chi_4^0}^2; m_t^2, m_{\tilde{t}_k}^2) + m_{\chi_4^0} B_1(m_{\chi_4^0}^2; m_t^2, m_{\tilde{t}_k}^2) \right\}, \tag{1.26}$$

which is an approximation for the top-stop loop contribution to δM_χ^{44}.

A.2 Bottom-sbottom loops in δM_χ

Bottom-sbottom loops contribute importantly to δM_χ, and through it, also contribute importantly to the third term in eq. (2.12). Bottom-sbottom loops contribute importantly

to δM_ν too, but they are not the focus of this study. The neutral fermion coupling to bottom-sbottom quarks is,

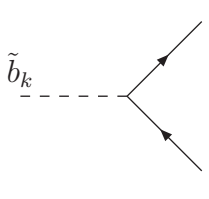

$$= i\left[O_{Ljk}^{bn\tilde{b}}\tfrac{(1-\gamma_5)}{2} + O_{Rjk}^{bn\tilde{b}}\tfrac{(1+\gamma_5)}{2}\right],$$

with

$$\begin{aligned} O_{Ljk}^{bn\tilde{b}} &= -\eta_j \frac{2gt_W}{3\sqrt{2}}\mathcal{N}_{j1}^* R_{k2}^{\tilde{b}} - \eta_j h_b \mathcal{N}_{j3}^* R_{k1}^{\tilde{b}}\,, \\ O_{Rjk}^{bn\tilde{b}} &= \frac{g}{\sqrt{2}}\left(\mathcal{N}_{j2} - \frac{1}{3}t_W\mathcal{N}_{j1}\right)R_{k1}^{\tilde{b}} - h_b\mathcal{N}_{j3}R_{k2}^{\tilde{b}}\,, \end{aligned} \tag{1.27}$$

and where h_b is the bottom quark Yukawa coupling, $R^{\tilde{b}}$ is the (assumed real) 2×2 rotation matrix that diagonalizes the sbottom quark mass matrix, $\mathcal{N}$ is the already defined (and real) 7×7 rotation matrix that diagonalizes the neutralino sector, and η_j is the already defined sign of the corresponding fermion j. Specializing this coupling to the case when the neutral fermion is a neutralino, one finds,

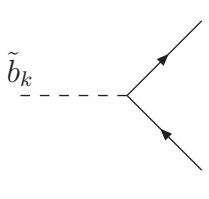

$$= i\left[O_{Ljk}^{b\chi\tilde{b}}\tfrac{(1-\gamma_5)}{2} + O_{Rjk}^{b\chi\tilde{b}}\tfrac{(1+\gamma_5)}{2}\right],$$

with

$$\begin{aligned} O_{Ljk}^{b\chi\tilde{b}} &= -\eta_j \frac{2gt_W}{3\sqrt{2}}N_{j1}^* R_{k2}^{\tilde{b}} - \eta_j h_b N_{j3}^* R_{k1}^{\tilde{b}}\,, \\ O_{Rjk}^{b\chi\tilde{b}} &= \frac{g}{\sqrt{2}}\left(N_{j2} - \frac{1}{3}t_W N_{j1}\right)R_{k1}^{\tilde{b}} - h_b N_{j3}R_{k2}^{\tilde{b}}\,, \end{aligned} \tag{1.28}$$

and where N is the already defined (real) 4×4 rotation matrix that diagonalizes the neutralino mass sub-matrix. The bottom-sbottom loops are,

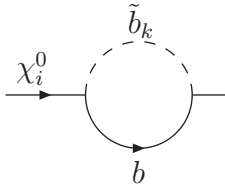

$$= i\,\Sigma_{ij}^{b\tilde{b}}(p^2),$$

where

$$\Sigma_{ij}^{b\tilde{b}}(p^2) = \frac{n_c h_b^2 N_{i3} N_{j3}}{16\pi^2} \sum_{k=1}^{2} \left[m_b R_{k1}^{\tilde{b}} R_{k2}^{\tilde{b}} (\eta_i P_L + \eta_j P_R) B_0^{p b\tilde{b}} - \not{p} (R_{k1}^{\tilde{b}2} \eta_i \eta_j P_L + R_{k2}^{\tilde{b}2} P_R) B_1^{p b\tilde{b}} \right] + ... \tag{1.29}$$

and again, only the terms proportional to h_b^2 are shown. The contribution to δM_χ^{ij} is therefore,

$$\begin{aligned}
\delta M_\chi^{ij} &= \frac{n_c h_b^2 N_{i3} N_{j3}}{32\pi^2} \sum_{k=1}^{2} \Bigg\{ -\frac{1}{2} m_b R_{k1}^{\tilde{b}} R_{k2}^{\tilde{b}} (\eta_i + \eta_j) \left(B_0^{\chi_i b\tilde{b}} + B_0^{\chi_j b\tilde{b}} \right) \\
&\qquad + \frac{1}{2} (R_{k1}^{\tilde{b}2} \eta_i \eta_j + R_{k2}^{\tilde{b}2}) \left(m_{\chi_i^0} B_1^{\chi_i b\tilde{b}} + m_{\chi_j^0} B_1^{\chi_j b\tilde{b}} \right) \Bigg\}, \\
&= \frac{n_c h_b^2 N_{i3} N_{j3}}{32\pi^2} \sum_{k=1}^{2} \Bigg\{ \frac{1}{2} m_b s_{\tilde{b}} c_{\tilde{b}} (-1)^k (\eta_i + \eta_j) \left(B_0^{\chi_i b\tilde{b}} + B_0^{\chi_j b\tilde{b}} \right) \\
&\qquad + \frac{1}{2} (c_{\tilde{b}}^2 \eta_i \eta_j + s_{\tilde{b}}^2) \left(m_{\chi_i^0} B_1^{\chi_i b\tilde{b}} + m_{\chi_j^0} B_1^{\chi_j b\tilde{b}} \right) \Bigg\}.
\end{aligned} \tag{1.30}$$

The contribution to the $(4,4)$ neutrino/neutralino mass matrix element is therefore,

$$\delta M_\chi^{44} = \frac{n_c h_b^2 N_{43}^2}{32\pi^2} \sum_{k=1}^{2} \left\{ 2 m_b s_{\tilde{b}} c_{\tilde{b}} (-1)^k \eta_4 B_0(m_{\chi_4^0}^2; m_b^2, m_{\tilde{b}_k}^2) + m_{\chi_4^0} B_1(m_{\chi_4^0}^2; m_b^2, m_{\tilde{b}_k}^2) \right\}, \tag{1.31}$$

which is an approximation for the bottom-sbottom loop contribution to δM_χ^{44}.

A.3 Top-stop loops in δm

In δm one has mixing between neutralinos and neutrinos. Therefore, to find the quantum corrections in this region of the mass matrix the neutralino-top-stop coupling in eq. (1.23) is needed. Also, to specialize the general coupling in eq. (1.22) to the neutrino-top-stop coupling is needed. One finds,

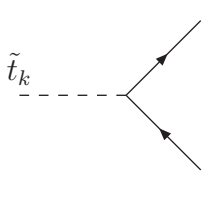

$$= i \left[O_{Ljk}^{t\nu\tilde{t}} \tfrac{(1-\gamma_5)}{2} + O_{Rjk}^{t\nu\tilde{t}} \tfrac{(1+\gamma_5)}{2} \right],$$

with

$$
\begin{aligned}
O^{t\nu\tilde{t}}_{Ljk} &= \eta_j R^{\tilde{t}}_{k1} h_t \xi_{j4} - \eta_j R^{\tilde{t}}_{k2} \frac{4 g t_W}{3\sqrt{2}} \xi_{j1} \equiv \eta_j \widetilde{O}^{t\nu\tilde{t}}_{Lk} \Lambda_j \,, \\
O^{t\nu\tilde{t}}_{Rjk} &= R^{\tilde{t}}_{k1} \frac{g}{\sqrt{2}} \left(\xi_{j2} + \frac{1}{3} t_W \xi_{j1} \right) + R^{\tilde{t}}_{k2} h_t \xi_{j4} \equiv \widetilde{O}^{t\nu\tilde{t}}_{Rk} \Lambda_j \,.
\end{aligned} \tag{1.32}
$$

In the last equalities, the $\widetilde{O}$ couplings are defined as,

$$
\begin{aligned}
\widetilde{O}^{t\nu\tilde{t}}_{Lk} &= R^{\tilde{t}}_{k1} h_t \xi_4 - R^{\tilde{t}}_{k2} \frac{4 g t_W}{3\sqrt{2}} \xi_1 \,, \\
\widetilde{O}^{t\nu\tilde{t}}_{Rk} &= R^{\tilde{t}}_{k1} \frac{g}{\sqrt{2}} \left(\xi_2 + \frac{1}{3} t_W \xi_1 \right) + R^{\tilde{t}}_{k2} h_t \xi_4 \,,
\end{aligned} \tag{1.33}
$$

and the ξ_{ij} and ξ_i parameters are defined in Appendix C. The loops contributing to δm are,

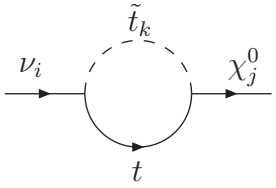

$= i\,\Sigma^{t\tilde{t}}_{i+4,j}(p^2),$

with

$$
\Sigma^{t\tilde{t}}_{i+4,j}(p^2) = -\frac{n_c h_t^2 \xi_{i4} N_{j4}}{16\pi^2} \sum_{k=1}^{2} \left[m_t R^{\tilde{t}}_{k1} R^{\tilde{t}}_{k2} (\eta_i P_L + \eta_j P_R) B_0^{pt\tilde{t}} - \not{p} (R^{\tilde{t}2}_{k1} \eta_i \eta_j P_L + R^{\tilde{t}2}_{k2} P_R) B_1^{pt\tilde{t}} \right] + ... \tag{1.34}
$$

where only terms proportional to the Yukawa coupling squared are kept. The above leads to the following contribution to δm,

$$
\begin{aligned}
\delta m^{t\tilde{t}}_{ij} &= \frac{n_c h_t^2 \xi_4 N_{j4}}{64\pi^2} \sum_{k=1}^{2} \Big\{ m_t s_{\tilde{t}} c_{\tilde{t}} (-1)^k \left(\eta_i + \eta_j \right) \left[B_0(m^2_{\chi^0_j}; m_t, m_{\tilde{t}_k}) + B_0(0; m_t, m_{\tilde{t}_k}) \right] \\
&\quad - m_{\chi^0_4} \left(\eta_i \eta_j c^2_{\tilde{t}} + s^2_{\tilde{t}} \right) B_1(m^2_{\chi^0_j}; m_t, m_{\tilde{t}_k}) \Big\} \Lambda_i \,.
\end{aligned} \tag{1.35}
$$

From this result one learns that the second order term in eq. (2.12) will never generate a solar neutrino mass from top-stop loops. This last conclusion arises because there is no term proportional to ϵ_i in eq. (1.35).

A.4 Bottom-sbottom loops in δm

As it was mentioned before, in δm one has mixing between neutralinos and neutrinos. The contribution from bottom-sbottom loops to this quantity starts with the neutral fermion coupling to bottom-sbottom quarks, which is given in eq. (1.27). Specializing that coupling to the case when the neutral fermion is a neutrino one finds,

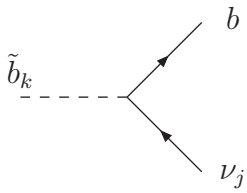

$$= i\left[O^{b\nu\tilde{b}}_{Ljk}\frac{(1-\gamma_5)}{2} + O^{b\nu\tilde{b}}_{Rjk}\frac{(1+\gamma_5)}{2}\right],$$

with

$$\begin{aligned} O^{b\nu\tilde{b}}_{Ljk} &= \eta_j\frac{2gt_W}{3\sqrt{2}}\xi_{j1}R^{\tilde{b}}_{k2} + \eta_j h_b\xi_{j3}R^{\tilde{b}}_{k1} \equiv \eta_j\widetilde{O}^{b\nu\tilde{b}}_{Lk}\,\Lambda_j - \eta_j\frac{h_b R^{\tilde{b}}_{k1}}{\mu}\epsilon_j\,, \\ O^{b\nu\tilde{b}}_{Rjk} &= -\frac{g}{\sqrt{2}}\left(\xi_{j2} - \frac{1}{3}t_W\xi_{j1}\right)R^{\tilde{b}}_{k1} + h_b\xi_{j3}R^{\tilde{b}}_{k2} \equiv \widetilde{O}^{b\nu\tilde{b}}_{Rk}\,\Lambda_j - \frac{h_b R^{\tilde{b}}_{k2}}{\mu}\epsilon_j\,. \end{aligned} \tag{1.36}$$

In the last equalities, the $\widetilde{O}$ couplings are defined as,

$$\begin{aligned} \widetilde{O}^{b\nu\tilde{b}}_{Lk} &= \frac{2gt_W}{3\sqrt{2}}\xi_1 R^{\tilde{b}}_{k2} + h_b\xi_3 R^{\tilde{b}}_{k1}\,, \\ \widetilde{O}^{b\nu\tilde{b}}_{Rk} &= -\frac{g}{\sqrt{2}}\left(\xi_2 - \frac{1}{3}t_W\xi_1\right)R^{\tilde{b}}_{k1} + h_b\xi_3 R^{\tilde{b}}_{k2}\,. \end{aligned} \tag{1.37}$$

In addition, the neutralino coupling to bottom-sbottom, given in eq. (1.28), is needed. The bottom-sbottom loops contributing to δm are therefore,

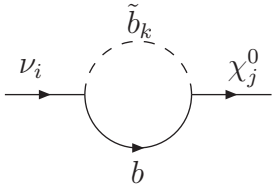

$$= i\,\Sigma^{b\tilde{b}}_{i+4,j}(p^2),$$

with

$$\Sigma^{b\tilde{b}}_{i+4,j}(p^2) = -\frac{n_c h_b^2\xi_{i3}N_{j3}}{16\pi^2}\sum_{k=1}^{2}\left[m_b R^{\tilde{b}}_{k1}R^{\tilde{b}}_{k2}(\eta_i P_L + \eta_j P_R)B_0^{pb\tilde{b}} - \not{p}(R^{\tilde{b}2}_{k1}\eta_i\eta_j P_L + R^{\tilde{b}2}_{k2}P_R)B_1^{pb\tilde{b}}\right] + ... \tag{1.38}$$

where again only terms proportional to the Yukawa coupling squared are kept. The above leads to the following contribution to δm,

$$\begin{aligned}
\delta m_{ij}^{b\tilde{b}} &= \frac{n_c h_b^2 \xi_3 N_{j3}}{64\pi^2} \sum_{k=1}^{2} \Big\{ m_b s_{\tilde{b}} c_{\tilde{b}} (-1)^k \left(\eta_i + \eta_j\right) \Big[B_0(m^2_{\chi^0_j}; m_b, m_{\tilde{b}_k}) + B_0(0; m_b, m_{\tilde{b}_k}) \Big] \\
&\qquad - m_{\chi^0_j} \left(\eta_i \eta_j c^2_{\tilde{b}} + s^2_{\tilde{b}}\right) B_1(m^2_{\chi^0_j}; m_b, m_{\tilde{b}_k}) \Big\} \Lambda_i \\
&\quad - \frac{n_c h_b^2 N_{j3}}{64\pi^2 \mu} \sum_{k=1}^{2} \Big\{ m_b s_{\tilde{b}} c_{\tilde{b}} (-1)^k \left(\eta_i + \eta_j\right) \Big[B_0(m^2_{\chi^0_j}; m_b, m_{\tilde{b}_k}) + B_0(0; m_b, m_{\tilde{b}_k}) \Big] \\
&\qquad - m_{\chi^0_j} \left(\eta_i \eta_j c^2_{\tilde{b}} + s^2_{\tilde{b}}\right) B_1(m^2_{\chi^0_j}; m_b, m_{\tilde{b}_k}) \Big\} \epsilon_i \equiv (\delta m^{b\tilde{b}}_{3,\Lambda}) \Lambda_i + (\delta m^{b\tilde{b}}_{3,\epsilon}) \epsilon_i \,. \qquad (1.39)
\end{aligned}$$

From this result one learns that the second order term in eq. (2.12) can generate a solar neutrino mass from bottom-sbottom loops, because of the term proportional to ϵ_i in eq. (1.39). But that fact is known. More importantly, one learns that the top-stop loops can contribute to the solar mass through the third order term in eq. (2.12), in combination with the bottom-sbottom loops.

B Inverse Neutralino Mass Matrix

For the reader's benefit, the inverse of the tree-level neutralino mass matrix is given. Its matrix elements are equal to,

$$(\mathrm{M}^0_\chi)^{-1} = \frac{1}{\det M_{\chi^0}} \begin{bmatrix} I^{gg} & I^{gh} \\ I^{hg} & I^{hh} \end{bmatrix}, \qquad (2.40)$$

with the following expressions for each sub-matrix,

$$\begin{aligned}
I^{gg} &= \begin{bmatrix} -M_2\mu^2 + \frac{1}{2}g^2 v_u v_d \mu & \frac{1}{2} g g' v_u v_d \mu \\ \frac{1}{2} g g' v_u v_d \mu & -M_1 \mu^2 + \frac{1}{2} g'^2 v_u v_d \mu \end{bmatrix}, \\
I^{gh} &= \begin{bmatrix} -\frac{1}{2} g' v_u M_2 \mu & \frac{1}{2} g' v_d M_2 \mu \\ \frac{1}{2} g v_u M_1 \mu & -\frac{1}{2} g v_d M_1 \mu \end{bmatrix}, \qquad (2.41) \\
I^{hh} &= \begin{bmatrix} -\frac{1}{4}(g^2 M_1 + g'^2 M_2) v_u^2 & M_1 M_2 \mu - \frac{1}{4}(g^2 M_1 + g'^2 M_2) v_u v_d \\ M_1 M_2 \mu - \frac{1}{4}(g^2 M_1 + g'^2 M_2) v_u v_d & -\frac{1}{4}(g^2 M_1 + g'^2 M_2) v_d^2 \end{bmatrix},
\end{aligned}$$

and $I^{hg} = (I^{gh})^T$.

C Approximated Neutralino/Neutrino Rotation Matrix

The neutralino/neutrino 7×7 mass matrix is diagonalized, in first approximation, by

$$\mathcal{N} \approx \begin{bmatrix} N & N\xi^T \\ -N_\nu \xi & N_\nu \end{bmatrix} \tag{3.42}$$

where N diagonalizes the 4×4 neutralino sub-matrix, N_ν diagonalizes the 3×3 neutrino sub-matrix, and the 3×4 matrix ξ is part of the block diagonalization described in eq. (2.4). The parameters $\xi_{ij} = (m\, \mathrm{M}_{\chi^0}^{-1})_{ij}$ are very important and have simple expressions,

$$\begin{aligned} \xi_{i1} &= \frac{g' M_2 \mu}{2 \det M_{\chi^0}} \Lambda_i \,, & \xi_{i2} &= \frac{g M_1 \mu}{2 \det M_{\chi^0}} \Lambda_i \,, \\ \xi_{i3} &= \frac{(g^2 M_1 + g'^2 M_2) v_u}{4 \det M_{\chi^0}} \Lambda_i - \frac{\epsilon_i}{\mu} \,, & \xi_{i4} &= -\frac{(g^2 M_1 + g'^2 M_2) v_d}{4 \det M_{\chi^0}} \Lambda_i \,. \end{aligned} \tag{3.43}$$

One defines also the reduce notation $\xi_{i1} = \xi_1 \Lambda_i$, $\xi_{i2} = \xi_2 \Lambda_i$, $\xi_{i3} = \xi_3 \Lambda_i - \epsilon_i/\mu$, and $\xi_{i4} = \xi_4 \Lambda_i$.

References

[1] [Kamiokande Collaboration]: Y. Fukuda *et al.*, Phys. Lett. B **335** (1994) 237; Phys. Rev. Lett. **77** (1996) 1683. S. Hatakeyama *et al.*, Phys. Rev. Lett. **81** (1998) 2016.

[2] [Super-Kamiokande Collaboration]: Y. Fukuda *et al.*, Phys. Rev. Lett. **81** (1998) 1562; Phys. Rev. Lett. **86** (2001) 5656; Phys. Rev. Lett. **86** (2001) 5651; Phys. Lett. B **539** (2002) 179; M. B. Smy *et al.*, Phys. Rev. D **69** (2004) 011104; Y. Ashie *et al.*, Phys. Rev. Lett. **93** (2004) 101801.

[3] [KamLAND Collaboration] K. Eguchi *et al.*, Phys. Rev. Lett. **90** (2003) 021802;
T. Araki *et al.*, Phys. Rev. Lett. **94** (2005) 081801.

[4] [K2K Collaboration] M. H. Ahn *et al.*, Phys. Rev. Lett. **90** (2003) 041801.
E. Aliu *et al.*, Phys. Rev. Lett. **94** (2005) 081802.

[5] [Soudan 2 Collaboration]: M. C. Sanchez *et al.*, Phys. Rev. D **68** (2003) 113004.

[6] [SNO Collaboration]: Q. R. Ahmad *et al.*, Phys. Rev. Lett. **87** (2001) 071301; Phys. Rev. Lett. **89** (2002) 011301;
Phys. Rev. Lett. **89** (2002) 011302; S. N. Ahmed *et al.*, Phys. Rev. Lett. **92** (2004) 181301.

[7] [SAGE Collaboration]: J. N. Abdurashitov *et al.*, J. Exp. Theor. Phys. **95** (2002) 181 [Zh. Eksp. Teor. Fiz. **122** (2002) 211].

[8] [GALLEX Collaboration]: W. Hampel *et al.*, Phys. Lett. B **447** (1999) 127.

[9] [MACRO Collaboration]: M. Ambrosio *et al.*, Phys. Lett. B **566** (2003) 35.
Eur. Phys. J. C **36** (2004) 323.

[10] K. Abe *et al.* [T2K Collaboration], Phys. Rev. Lett. **107** (2011) 041801.

[11] P. Adamson *et al.* [MINOS Collaboration], Phys. Rev. Lett. **108** (2012) 191801.

[12] F. P. An *et al.* [DAYA-BAY Collaboration], Phys. Rev. Lett. **108** (2012) 171803.

[13] J. K. Ahn *et al.* [RENO Collaboration], Phys. Rev. Lett. **108** (2012) 191802.

[14] Y. Abe *et al.* [DOUBLE-CHOOZ Collaboration], Phys. Rev. Lett. **108** (2012) 131801; Phys. Rev. D **86** (2012) 052008.

[15] D. V. Forero, M. Tortola and J. W. F. Valle, Phys. Rev. D **86** (2012) 073012 G. L. Fogli, E. Lisi, A. Marrone, D. Montanino, A. Palazzo and A. M. Rotunno, Phys. Rev. D **86** (2012) 013012. M. C. Gonzalez-Garcia, M. Maltoni, J. Salvado and T. Schwetz, JHEP **1212** (2012) 123.

[16] H. E. Haber and G. L. Kane, Phys. Rept. **117** (1985) 75.

[17] G. R. Farrar and P. Fayet, Phys. Lett. B **76** (1978) 575; S. Dimopoulos and H. Georgi, Nucl. Phys. B **193** (1981) 150; L. J. Hall and M. Suzuki, Nucl. Phys. B **231** (1984) 419; L. E. Ibanez and G. G. Ross, Nucl. Phys. B **368** (1992) 3.

[18] R. Barbier *et al.*, Phys. Rept. **420** (2005) 1.

[19] M. A. Diaz, J. C. Romao and J. W. F. Valle, Nucl. Phys. B **524**, 23 (1998).

[20] M. Hirsch, M. A. Diaz, W. Porod, J. C. Romao and J. W. F. Valle, Phys. Rev. D **62**, 113008 (2000) [Erratum-ibid. D **65**, 119901 (2002)] [hep-ph/0004115].

[21] M. A. Diaz, M. Hirsch, W. Porod, J. C. Romao and J. W. F. Valle, Phys. Rev. D **68**, 013009 (2003) [Erratum-ibid. D **71**, 059904 (2005)] [hep-ph/0302021].

[22] S. Chatrchyan *et al.* [CMS Collaboration], Phys. Rev. Lett. **107**, 221804 (2011) [arXiv:1109.2352 [hep-ex]]. G. Aad *et al.* [ATLAS Collaboration], Phys. Lett. B **710**, 67 (2012) [arXiv:1109.6572 [hep-ex]].

[23] R. Hempfling, Nucl. Phys. B **478**, 3 (1996) [hep-ph/9511288].

[24] W. Porod, M. Hirsch, J. Romao and J. W. F. Valle, Phys. Rev. D **63**, 115004 (2001) [hep-ph/0011248]; M. A. Diaz, R. A. Lineros and M. A. Rivera, Phys. Rev. D **67**, 115004 (2003).

[25] H. Minakata, H. Nunokawa, W. J. C. Teves and R. Zukanovich Funchal, Phys. Rev. D **71**, 013005 (2005): J. P. Cravens *et al.* [Super-Kamiokande Collaboration], Phys. Rev. D **78** (2008) 032002.

[26] J. M. Mira, E. Nardi, D. A. Restrepo and J. W. F. Valle, Phys. Lett. B **492**, 81 (2000) [hep-ph/0007266].

[27] M. Hirsch, J. C. Romao and J. W. F. Valle, Phys. Lett. B **486** (2000) 255 [hep-ph/0002264].

[28] A. Djouadi, J. -L. Kneur and G. Moultaka, Comput. Phys. Commun. **176** (2007) 426 [hep-ph/0211331].

[29] G. Aad *et al.* [ATLAS Collaboration], Phys. Lett. B **716**, 1 (2012) [arXiv:1207.7214 [hep-ex]]; S. Chatrchyan *et al.* [CMS Collaboration], Phys. Lett. B **716**, 30 (2012) [arXiv:1207.7235 [hep-ex]].

[30] J. Beringer *et al.* [Particle Data Group Collaboration], Phys. Rev. D **86**, 010001 (2012).

[31] D. A. Ross and M. J. G. Veltman, Nucl. Phys. B **95**, 135 (1975).

[32] G. W. Bennett *et al.* [Muon G-2 Collaboration], Phys. Rev. D **73**, 072003 (2006) [hep-ex/0602035].

[33] D. Asner *et al.* [Heavy Flavor Averaging Group Collaboration], arXiv:1010.1589 [hep-ex].

[34] R.Y. Rubinstein, D.P. Kroese, "Simulation and the Monte Carlo Method", Wiley Series in Probability and Statistics (2007).

[35] G. Aad *et al.* [ATLAS Collaboration], JHEP **1406**, 035 (2014) [arXiv:1404.2500 [hep-ex]]; G. Aad *et al.* [ATLAS Collaboration], JHEP **1405**, 071 (2014) [arXiv:1403.5294 [hep-ex]]; G. Aad *et al.* [ATLAS Collaboration], arXiv:1405.5086 [hep-ex]; G. Aad *et al.* [ATLAS Collaboration], JHEP **1406**, 035 (2014) [arXiv:1404.2500 [hep-ex]]; G. Aad *et al.* [ATLAS Collaboration], Phys. Lett. B **723**, 15 (2013) [arXiv:1212.1272].

[36] [CMS Collaboration], CMS-PAS-SUS-12-027; S. Chatrchyan *et al.* [CMS Collaboration], Phys. Rev. Lett. **111**, no. 22, 221801 (2013) [arXiv:1306.6643 [hep-ex]]; S. Chatrchyan *et al.* [CMS Collaboration], Phys. Lett. B **730**, 193 (2014) [arXiv:1311.1799 [hep-ex]].